# Full orbit computations of ripple-induced fusion $\alpha$-particle losses from burning tokamak plasmas

K. G. McClements

*EURATOM/UKAEA Fusion Association, Culham Science Centre, Abingdon, Oxfordshire OX14 3DB, United Kingdom*

A full orbit code is used to compute collisionless losses of fusion $\alpha$ particles from three proposed burning plasma tokamaks: the International Tokamak Experimental Reactor (ITER); a spherical tokamak power plant (STPP) [T. C. Hender, A. Bond, J. Edwards, P. J. Karditsas, K. G. McClements, J. Mustoe, D. V. Sherwood, G. M. Voss, and H. R. Wilson, Fusion Eng. Des. **48**, 255 (2000)]; and a spherical tokamak components test facility (CTF) [H. R. Wilson, G. M. Voss, R. J. Akers, L. Appel, A. Dnestrovskij, O. Keating, T. C. Hender, M. J. Hole, G. Huysmans, A. Kirk, P. J. Knight, M. Loughlin, K. G. McClements, M. R. O'Brien, and D. Yu. Sychugov, *Proceedings of the 20th IAEA Fusion Energy Conference*, Invited Paper FT/3-1Ra]. It has been suggested that $\alpha$ particle transport could be enhanced due to cyclotron resonance with the toroidal magnetic field ripple. However, calculations for inductive operation in ITER yield a loss rate that appears to be broadly consistent with the predictions of guiding center theory, falling monotonically as the number of toroidal field coils $N$ is increased (and hence the ripple amplitude is decreased). For STPP and CTF the loss rate does not decrease monotonically with $N$, but collisionless losses are generally low in absolute terms. As in the case of ITER, there is no evidence that finite Larmor radius effects would seriously degrade fusion $\alpha$-particle confinement. [DOI: 10.1063/1.1936532]

## I. INTRODUCTION

Due to the discrete nature of its toroidal field coils, a tokamak cannot have a perfectly axisymmetric equilibrium magnetic field. In general, the departures from perfect axisymmetry have an adverse effect on the confinement of energetic particles, including fusion $\alpha$ particles. Ripple losses of fusion $\alpha$ particles are of concern first because they reduce the extent to which such particles can heat the plasma (i.e., the ignition margin) and second because the associated particle and heat fluxes may damage plasma-facing components. For these reasons, ripple-induced $\alpha$-particle losses from the proposed burning tokamak plasmas, in particular, the International Tokamak Experimental Reactor (ITER), have been modeled by many authors.[1–9] Specific mechanisms likely to determine fast particle transport in the presence of toroidal field ripple have also been investigated extensively.[10–14] In most of these studies, the treatment of fast particle transport has been based on guiding center theory. However, Hinton[12] and Putvinskii and co-workers[13,14] have also examined the possibility that a fast particle cyclotron resonance with the ripple field could give rise to additional transport and loss. The resonance condition is[3]

$$k_{\parallel} v_{\parallel} = \Omega_{\alpha}, \tag{1}$$

where $k_{\parallel}$ is the ripple wave vector component parallel to the local magnetic field, $v_{\parallel}$ is the parallel component of the $\alpha$-particle velocity, and $\Omega_{\alpha}$ is the $\alpha$-particle cyclotron frequency. Cyclotron effects are thus expected to become important when the ripple wavelength divided by $2\pi$ is comparable to the $\alpha$-particle Larmor radius. The ITER design has $N=18$ toroidal field coils and major radius $R \simeq 6$ m, giving $k_{\parallel}^{-1} \simeq 0.3$ m, while fusion $\alpha$ particles would be born with

Larmor radii of around 5 cm. This appears to indicate that cyclotron effects on ripple losses are likely to be negligible in ITER. However, it has been proposed that ferromagnetic inserts be used in this device to reduce the ripple amplitude and thereby to minimize $\alpha$-particle losses.[7] In addition to reducing the ripple amplitude, such inserts have the effect of introducing shorter length scales into the ripple field. This reopens the issue of whether cyclotron effects could play a role in $\alpha$-particle transport. Another key motivation for reexamining full orbit effects on ripple losses is that designs have been proposed for burning plasma experiments based on the spherical tokamak concept.[15–18] The combination of low $R$ and low magnetic field in such devices makes it much more likely that cyclotron resonance effects will be significant.

In this paper we use a full orbit code CUlham Energy-conserving orBIT (CUEBIT) (Ref. 19) to compute losses of fusion $\alpha$ particles from ITER, a proposed spherical tokamak power plant (STPP),[15] and a proposed spherical tokamak components test facility (CTF).[18] For this purpose we first construct a solution for the ripple field that is separable in $R$ and height $Z$ (Sec. II). After presenting the computed loss rates for the three devices (Sec. III), we then discuss possible interpretations of the results (Sec. IV).

## II. MODEL OF RIPPLE FIELD

In common with previous authors, we assume that the toroidal field ripple $\widetilde{\mathbf{B}}$ is determined solely by currents outside the plasma, and is thus described by the vacuum Maxwell equations

$$\boldsymbol{\nabla} \cdot \widetilde{\mathbf{B}} = 0, \tag{2}$$

**12**, 072510-1

$$\nabla \times \widetilde{\mathbf{B}} = \mathbf{0}. \tag{3}$$

The two spherical tokamaks considered in this paper (STPP and CTF) are characterized by relatively high values of plasma beta ($\beta \sim 1$). It is important to check that the ripple field can be accurately represented by the vacuum Maxwell equations in such cases. For simplicity, we model the ripple as a poloidally symmetric perturbation to a cylindrical plasma with uniform axial magnetic field. The radial plasma displacement $\xi$ that minimizes the potential energy associated with the perturbation satisfies the Euler–Lagrange equation[20]

$$\frac{d}{dr}\left(r\frac{d\xi}{dr}\right) - \left(\frac{d\beta}{dr} + \frac{k^2r^2+1}{r}\right)\xi = 0, \tag{4}$$

where $r$ is distance from the cylinder axis and $k$ is the wave number of the ripple perturbation. Putting $k=N/R$, we infer from Eq. (4) that the solution for $\xi$ and hence for the field perturbation is affected by the plasma beta only if

$$r\frac{d\beta}{dr} \sim \beta \gtrsim N^2 \epsilon^2, \tag{5}$$

where $\epsilon = r/R$. In all tokamaks $N^2 \gg 1$, and tokamaks with the highest values of $\beta$ are spherical tokamaks, for which $\epsilon \sim 1$ over most of the plasma cross section. Thus, Eq. (5) is unlikely ever to be satisfied, except possibly in a region very close to the magnetic axis. The ripple amplitude in this region is generally very low, and so fusion $\alpha$ particles born there are unlikely to undergo significant ripple transport. We conclude that the use of Eqs. (2) and (3) to model the ripple field is fully justified even in the high $\beta$ regime of spherical tokamaks.

The appropriate ripple solutions of Eqs. (2) and (3) are determined in general by the geometry of the coils and the currents flowing in them. Yushmanov[3] obtained an analytical solution for the case of circular coils. All of the devices considered in this paper have coils that are highly noncircular, and so the solution of Yushmanov is not strictly applicable. However, in most of our simulations we follow Yushmanov and other authors in assuming that the ripple can be well represented by a single toroidal harmonic, i.e., we assume that

$$\widetilde{B}_\varphi \propto \cos(N\varphi), \tag{6}$$

where $\varphi$ is toroidal angle, $\widetilde{B}_\varphi$ is the ripple perturbation to the toroidal field component, and $N$ is the number of toroidal field coils. In general, the ripple field contains a series of harmonics $\ell N$ where $\ell$ is an integer. However, calculations generally show that only the fundamental ($\ell = 1$) is significant inside the plasma.

We also follow Yushmanov in writing

$$\widetilde{B}_\varphi = \frac{B_0 R_0}{R}\delta(R,Z)\cos(N\varphi), \tag{7}$$

where $R$ is the distance from the tokamak symmetry axis, $Z$ is the vertical distance, $B_0$ and $R_0$ are constants, and $\delta$ is a function to be determined. Equation (2) indicates that the $R$ and $Z$ components of $\widetilde{\mathbf{B}}$ are of the form

$$\widetilde{B}_R = \frac{B_0 R_0}{R}\delta_R(R,Z)\sin(N\varphi), \tag{8}$$

$$\widetilde{B}_Z = \frac{B_0 R_0}{R}\delta_Z(R,Z)\sin(N\varphi). \tag{9}$$

Substituting these expressions into Eq. (3), we infer that

$$\delta_Z = \frac{R}{N}\frac{\partial\delta}{\partial Z}, \tag{10}$$

$$\delta_R = \frac{R}{N}\frac{\partial\delta}{\partial R}. \tag{11}$$

To obtain an equation for $\delta$, we use Eqs. (10) and (11) to eliminate $\delta_Z$ and $\delta_R$ from $\nabla \cdot \widetilde{\mathbf{B}} = 0$. This yields a Laplace-type equation of the form

$$\frac{1}{R}\frac{\partial}{\partial R}\left(R\frac{\partial\delta}{\partial R}\right) + \frac{\partial^2\delta}{\partial Z^2} - \frac{N^2}{R^2}\delta = 0. \tag{12}$$

As noted above, the three conceptual tokamaks modeled in this paper all have toroidal field coils that are highly noncircular. Indeed, as shown in Fig. 1 of Ref. 7, contours of constant ripple amplitude in the $(R,Z)$ plane computed numerically for ITER with ferromagnetic inserts taken into account more closely resemble elongated rectangles than circles. In the case of STPP, as shown in Fig. 2 of Ref. 15, the departure of numerically computed ripple contours from circularity is even more extreme, in that the ripple amplitude inside the plasma varies *only* with $R$.

Under these circumstances, it is appropriate to seek solutions of Eq. (12) that are separable in $R$ and $Z$:

$$\delta = f(R)g(Z). \tag{13}$$

Substituting this into Eq. (12) and dividing throughout by $fg$ we obtain

$$\frac{1}{Rf}\frac{d}{dR}(Rf') - \frac{N^2}{R^2} = -\frac{g''}{g}. \tag{14}$$

Each side of this equation must equal a constant; since the ripple field generally increases monotonically with $|Z|$, it is logical to choose negative values of this constant. Thus we write

$$g'' = \alpha^2 g. \tag{15}$$

For the case of an up-down symmetric ripple field, Eq. (15) has solution

$$g \propto \cosh(\alpha Z). \tag{16}$$

Noting that the equation for $f$ can be written in the form

$$\frac{d^2f}{dR^2} + \frac{1}{R}\frac{df}{dR} + \left(\alpha^2 - \frac{N^2}{R^2}\right)f = 0, \tag{17}$$

we deduce that

$$f \propto J_N(\alpha R), \tag{18}$$

where $J_N$ is the Bessel function of order $N$. The full solution is thus of the form

$$\delta(R,Z) = \delta_0 \cosh(\alpha Z) J_N(\alpha R), \tag{19}$$

where $\delta_0$ is a constant to be determined.

In the case of ITER, as noted previously, the number of coils $N$ is equal to 18. To estimate $\alpha$ in this case, we note from Fig. 1 in Ref. 5 that for values of $R$ close to that of the magnetic axis, $\delta$ increases by a factor of 10 between $Z \simeq 2.6$ m and $Z \simeq 3.8$ m. This implies $\alpha \simeq 2$; the function $J_N(\alpha R)$ is then monotonically increasing with $R$ beyond the last closed flux surface in the midplane. Consequently, the rise in ripple amplitude from the plasma center to the inboard plasma edge in ITER cannot be represented by a single separable solution. However, on the outboard side the variation of $\delta$ with $R$ is well represented by $J_N(\alpha R)$ with $\alpha = 2$. Since almost all ripple-induced $\alpha$-particle losses from burning tokamaks are predicted to occur on the outboard side of the plasma (see, e.g., Fig. 2 in Ref. 1), the fact that Eq. (18) is not applicable on the inboard side of ITER is unlikely to be important. The assumption of separability makes it possible to obtain a simple functional representation of the ripple field that satisfies the vacuum Maxwell equations and can be used to obtain scalings of $\alpha$-particle loss rates with ripple parameters, in particular, the number of toroidal field coils. In previous analyses of ripple losses from burning plasmas (e.g., Ref. 6), numerically determined ripple fields have typically been approximated by analytical expressions that in general do not satisfy Eqs. (2) and (3) and cannot be readily scaled to scenarios with different ripple parameters. As we will demonstrate in the following section, computing the $\alpha$-particle loss rate as a function of $N$, keeping other parameters fixed, is a useful method of identifying effects specifically associated with cyclotron motion.

We note finally that the model of the ITER ripple field discussed above could be improved, if necessary, by superposing two or more separable solutions. In particular, one could then model the rise in ripple amplitude from the plasma center to the inboard edge. With $\alpha^2$ in Eq. (15) taken to be negative, the appropriate solutions of Eq. (17) are modified Bessel functions of the second kind.

## III. COMPUTED LOSS RATES

### A. ITER

For the purpose of computing ripple losses of $\alpha$ particles, an ITER-like equilibrium generated using the Self-Consistent Equilibria with Neoclassical Effects (SCENE) code[21] was used. This equilibrium corresponds to the inductive mode of operation, with positive magnetic shear throughout the plasma. Previous guiding center calculations of $\alpha$-particle losses for this scenario, including collisional effects, indicate a particle loss rate of 2.15% without ferromagnetic inserts, and negligible losses with such inserts.[7]

Figure 1 shows the full orbit of a barely trapped 3.5 MeV $\alpha$ particle computed using CUEBIT for the ITER equilibrium. It is clear from this figure that the $\alpha$-particle Larmor radius is very small in relation to the size of the device. A quasirandom number generator was used to select $\alpha$-particle birth positions and velocity directions, assuming an isotropic pitch angle distribution and a distribution in poloidal flux
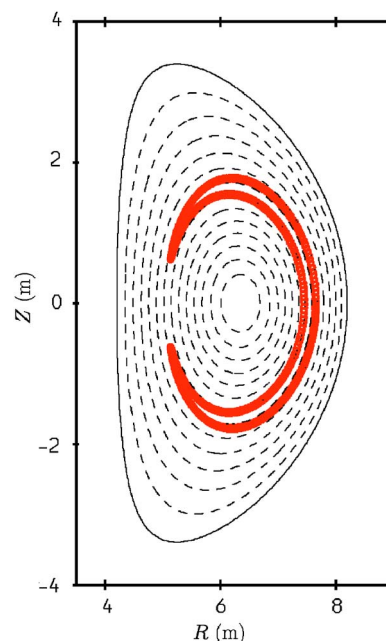


FIG. 1. Orbit of a barely trapped 3.5 MeV $\alpha$ particle in ITER. Flux surfaces are indicated by broken curves and the last closed flux surface by a solid curve.

proportional to the square of the pressure $p$ used to generate the equilibrium (the fusion reaction rate varies roughly as $p^2$ at ITER-relevant temperatures). The orbits of about 1400 $\alpha$ particles were followed for $\approx 10^5$ Larmor gyrations (corresponding to around 200 trapped particle bounce orbits). By recording the times at which particles were lost, it was found that this was sufficiently long for essentially all collisionless losses to occur. The ripple field was modeled using the parameters listed in the preceding section, with the number of toroidal field coils being varied from 16 to 20. The constant $\delta_0$ in Eq. (19) was chosen to ensure that the maximum absolute ripple amplitude inside the last closed flux surface was comparable to that predicted for ITER with $N=18$ in the absence of ferromagnetic inserts. A particle was deemed to be lost if at any instant it crossed the boundary of the computational domain used to generate the equilibrium.

The results are shown in Fig. 2; error bars in this figure are based on the assumption that computed loss rates obey Poisson statistics. In the vast majority of cases, $\alpha$ particles exiting the plasma do so vertically, in the direction of the grad-$B$ drift. The proportion of $\alpha$ particles that are lost before they complete a single banana orbit (i.e., the prompt loss rate) is indicated by a broken line (0.16%). As expected, the loss rate decreases monotonically as the number of coils is increased, i.e., as the ripple amplitude is reduced. There is no evidence of an enhancement in the loss rate at short ripple wavelengths due to cyclotron effects. For the number of coils in the ITER design ($N=18$), the loss rate is below 1%. This is somewhat lower than the figure of 2.15% obtained by Konovalov and co-workers,[7] made on the basis of guiding center calculations, but these calculations take into account collisional effects that enhance the loss rate. As discussed in Ref. 16, collisions can be readily incorporated into CUEBIT, but the need to resolve the full Larmor orbit with satisfactory
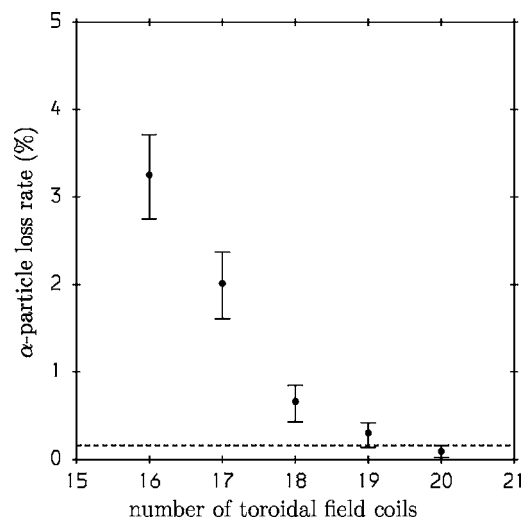
FIG. 2. Computed fusion $\alpha$ particle loss rate from ITER vs number of toroidal field coils. Particle orbits were computed for $\approx 10^5$ Larmor gyrations. The prompt loss rate is indicated by a broken line.

conservation of toroidal canonical momentum in the axisymmetric limit makes it computationally very demanding to simulate a large number of particles over a collisional slowing-down time. Accordingly, we consider only collisionless losses in this paper.

As discussed in Sec. I, the addition of ferromagnetic inserts means that the ripple field in ITER cannot necessarily be described by a single harmonic. To simulate the effect of additional harmonics, we repeated the loss calculation for the case of $N = 18$ with the $\cos(18\varphi)$ factor in Eq. (7) replaced by $\cos(18\varphi) + \cos(120\varphi)/2$, and similar modifications to $\widetilde{B}_R$ and $\widetilde{B}_Z$. The harmonic number of the additional term ($N = 120$) was chosen on the basis that the cyclotron resonance condition [Eq. (1)] is then approximately satisfied for a 3.5 MeV $\alpha$ particle. The normalization parameter $\delta_0$ was reduced so that the maximum amplitude was identical to that in the single harmonic case. Such a field does not satisfy the vacuum Maxwell equations, and must therefore be regarded as artificial: in general, higher harmonics of the ripple field tend to have relatively low amplitudes inside the plasma.[3] The assumed variation with $\varphi$, $R$, and $Z$ can thus be regarded as a worst case scenario. The computed loss rate in this case is very low ($0.4\% \pm 0.2\%$); within the large statistical uncertainty, it is identical to the figure obtained with a single harmonic (the $N = 18$ case in Fig. 2).

## B. The STPP

Hender and co-workers[15] presented outline engineering designs of a STPP, based on two alternative concepts for the central rod of the toroidal field circuit. More recently, Wilson and co-workers[16] have published the results of integrated plasma physics modeling for such a device. The toroidal field at the magnetic axis would be about 1 T. Figure 3 shows the orbit of a trapped 3.5 MeV particle in STPP; the solid straight lines indicate the location of the vacuum vessel wall. Although it is apparent that the normalized Larmor radius is larger than that of $\alpha$ particles in ITER (cf. Fig. 1), the pres-
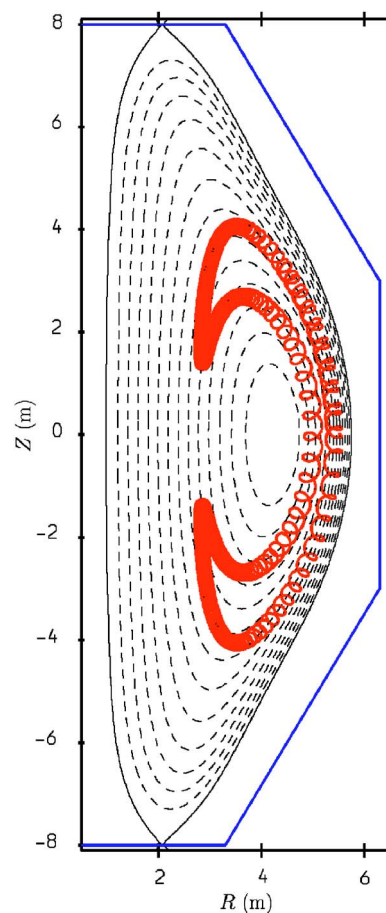


FIG. 3. Orbit of a trapped 3.5 MeV $\alpha$ particle in STPP. Flux surfaces are indicated by broken curves and the last closed flux surface by a solid curve. The solid straight lines indicate the location of the vacuum vessel wall.

ence of a relatively large poloidal field in the outer midplane reduces the orbit width to a value comparable to the Larmor radius. This pinching effect leads to an improvement in $\alpha$-particle confinement.[16]

As discussed in Sec. II, numerical computations of the STPP ripple field inside the last closed flux surface indicate that this depends only on $\varphi$ and $R$, not on $Z$. Taking the limit $\alpha \to 0$ in Eq. (19), we obtain $\delta \sim R^N$ and $\delta_R \sim R^N$. An appropriate choice for the proportionality constant is $1/R_{\text{coil}}^N$ where $R_{\text{coil}}$ is the radial location of the coils, i.e.,

$$\delta = \left(\frac{R}{R_{\text{coil}}}\right)^N. \qquad (20)$$

The numerically determined contours in Fig. 2 of Ref. 15, corresponding to $N = 16$, indicate that Eq. (20) is an accurate expression for the ripple field inside the last closed flux surface. With this model of $\delta$, the collisionless $\alpha$-particle loss rate was computed for values of $N$ ranging from 11 to 20: the results are shown in Fig. 4, together with the prompt loss rate. The properties of the axisymmetric part of the equilibrium used in this study are described in Ref. 16. The orbits of almost 5000 $\alpha$ particles were followed for $\approx 10^5$ Larmor gyrations (corresponding in this case to around $10^3$ trapped particle bounces). The $\alpha$-particle birth positions and velocities were again chosen quasirandomly from an isotropic
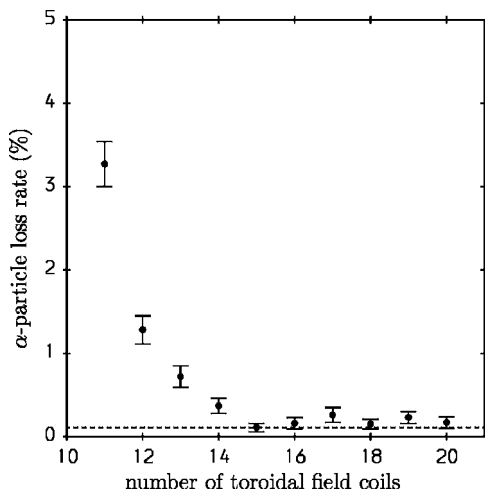
FIG. 4. Computed fusion $\alpha$-particle loss rate from STPP vs number of toroidal field coils. The $\alpha$-particle birth profile was assumed to be proportional to the square of the pressure. Particle orbits were computed for $\approx 10^5$ Larmor gyrations. The prompt loss rate is indicated by a broken line.



FIG. 5. As Fig. 4 except that the $\alpha$-particle birth profile in STPP was modeled using the Brysk cross section [Eq. (21)].

pitch angle distribution, with the birth probability again assumed to be proportional to the square of the pressure. In computing the loss rate, an $\alpha$ particle was deemed to be lost if at any instant it encountered the vacuum vessel wall shown in Fig. 3.

For low values of $N (\leqslant 15)$ the loss rate is a monotonic decreasing function of this parameter: in the case of $N=15$ all of the losses appear to be prompt. However, a further increase in the number of coils causes a slight degradation in $\alpha$-particle confinement. In particular, the losses for $N=17$ and $N=19$ are greater than the prompt rate. A crude estimate based on Eq. (1) indicates that cyclotron effects on $\alpha$-particle losses might be expected for $N \gtrsim 16$. It is interesting to note that the prompt loss rate (0.11%) is actually lower in STPP than it is in ITER (0.16%), despite the higher normalized $\alpha$-particle Larmor radius in the former; this appears to be due to the orbit pinching effect noted earlier.

Loss calculations were also carried out using a birth profile in poloidal flux based on the cross section obtained by Brysk[22] for thermal fuel ions at temperature $T$:

$$\langle \sigma v \rangle \propto \frac{1}{T^{2/3}} \exp\left[ -\frac{20}{T^{1/3}} \right], \tag{21}$$

where $T$ is in keV. In this case both temperature and density profiles are required in order to evaluate the $\alpha$-particle birth probability. The profile corresponding by Eq. (21) deviates significantly from the $n^2 T^2$ profile assumed previously at high temperature: the use of these two alternative models makes it possible to gauge the sensitivity of the loss rate calculations to plasma parameters. Results obtained using the Brysk cross section (Fig. 5) are qualitatively similar to those based on the $p^2$ profile (Fig. 4), but the value of $N$ for which losses drop to the prompt rate is now 16 (the number of coils in the base line STPP design) rather than 15. The loss rates for $N=13$, 14, 15, and 17 are indistiguishable (within the statistical uncertainty), despite the fact that the ripple amplitude at the outer midplane edge is about four times lower for $N=17$ than it is for $N=13$. There is no evidence of a further
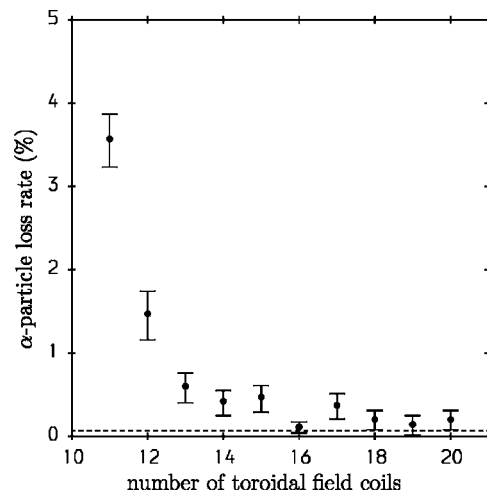
degradation in $\alpha$-particle confinement when $N$ is increased beyond the range considered in Fig. 5—the loss rate for $N=25$ is found to be similar to that for $N=18-20$.

**C. The CTF**

Wilson and co-workers[17,18] have recently explored the feasibility of developing a spherical tokamak for the specific purpose of testing components under conditions similar to those in a fusion power plant. The ratio of fusion power to supplied power envisaged for this CTF is $Q \simeq 1$, so that the conditions would approach those of a burning plasma. In the base line design there are ten toroidal field coils, located at a major radius of about 2.4 m. The toroidal field at the magnetic axis (about 2.8 T) would be somewhat larger than that in STPP, but the greater compactness of the device (major radius $R=0.75$ m) means that the normalized fusion $\alpha$-particle Larmor radius would be much higher; this is illustrated by the trapped orbit plotted in Fig. 6. The orbit pinching characteristic of spherical tokamaks is again apparent. One would expect $\alpha$-particle transport in this device to be affected by cyclotron resonance; Eq. (1) implies that such effects are likely to be important when $N \gtrsim 8$.

We have computed the $\alpha$-particle loss rate for $N$ in the range 7–20, with a birth profile modeled on the same basis as that used for ITER and STPP (i.e., the probability of a particle being born on a particular flux surface was taken to be proportional to the square of the plasma pressure on that surface). The axisymmetric part of the model equilibrium was that used in Ref. 18. A particle was assumed to be lost if it encountered any of the plasma-facing components. Between 2000 and 2500 particles were simulated for $10^5$ Larmor orbits (equivalent to several thousand trapped particle bounce orbits). The variation of loss rate with $N$ (Fig. 7) is qualitatively similar to that found in STPP: $\alpha$-particle confinement improves as $N$ is increased from 7 to 10, but we obtain similar loss rates for $N$ ranging from 10 to 20, despite a drop in the ripple amplitude at the outer midplane edge of about three orders of magnitude between these two values. Simulating $10^5$ Larmor orbits with a strictly axisymmetric
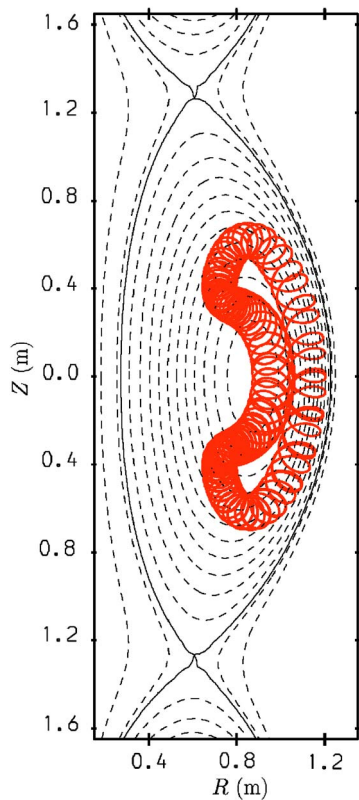
FIG. 6. Orbit of a trapped 3.5 MeV $\alpha$ particle in CTF. Flux surfaces are indicated by broken curves and the last closed flux surface by a solid curve.

field ($N \to \infty$), we obtain a lost fraction that is only slightly higher than the prompt rate. As in STPP, there are indications of improved confinement at one or possibly more intermediate values of $N$ (particularly $N=18$), although statistical errors make this somewhat less clear-cut than was the case in Figs. 4 and 5.

Computing the full trajectories of lost particles, we find that some of the losses are of particles that are initially in circulating orbits. For the case of $N=20$, Fig. 8 shows the full orbits of a trapped promptly lost particle (left) and an
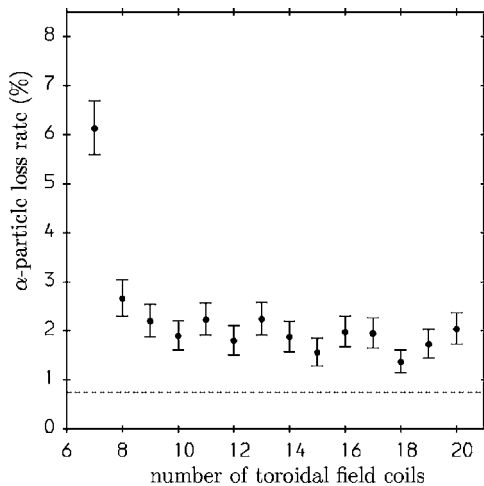


FIG. 7. Computed fusion $\alpha$-particle loss rate from CTF vs number of toroidal field coils. Particle orbits were computed for $\approx 10^5$ Larmor gyrations. The prompt loss rate is indicated by a broken line.
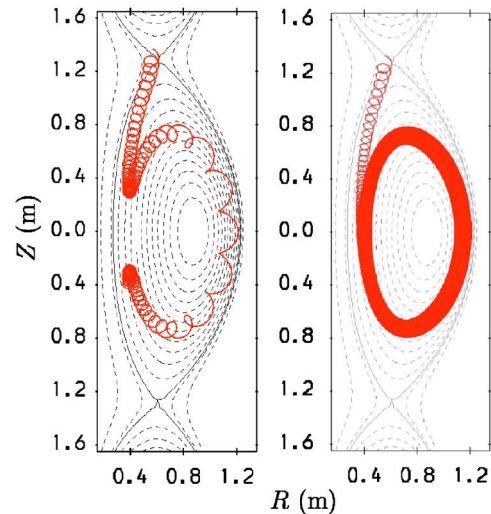


FIG. 8. Orbits of $\alpha$ particles lost from CTF with $N=20$. The left plot shows the prompt loss of a trapped particle; the right plot shows the delayed loss of an initially passing particle.

initially passing particle that is scattered into a trapped orbit and subsequently lost (right). Yushmanov[3] predicted that fast particle transport due to cyclotron resonance would not be restricted to trapped particles. It is not clear, however, that the loss shown in the right-hand plot is due specifically to the presence of magnetic field ripple: Yavorskij and co-workers[23] have shown that pitch angle scattering between the trapped and passing regions of velocity space can occur due to cyclotron effects even in the axisymmetric limit. Such scattering is associated with stochastic variations in magnetic moment $\mu$. Computing $\mu$ for a particle close to the trapped-passing boundary, we obtain the results shown in Fig. 9. In the top plot $N=14$; in the bottom plot $N \to \infty$. It is evident that $\mu$ varies stochastically in both cases, although the overall variation is somewhat greater in the case of $N=14$. The algorithm used in CUEBIT ensures that the energy of a charged particle in an arbitrary static magnetic field configuration is conserved to machine accuracy.[19] Satisfactory conservation of toroidal canonical momentum $P_\varphi$ in the axisymmetric limit can be achieved in the code by taking a sufficiently small time step: in the case of the time series shown in the lower frame of Fig. 9 (i.e., the axisymmetric case), $P_\varphi$ was conserved to an accuracy of about one part in $10^5$. It may be inferred from this that the stochastic variation of magnetic moment shown in Fig. 9 is physical rather than numerical. Similar variations of magnetic moment were found by Hastie and co-workers[24] for a nonadiabatic charged particle in a quadrupole field.

We have also examined the scaling of $\alpha$-particle losses with $N$ in CTF when the ripple amplitude at the outer midplane plasma edge is held fixed. It is evident from Eq. (20) that this requires $R_{coil}$ to be varied: in such a scan the ripple amplitude can only be clamped at one particular major radius. The amplitude $\delta$ at the outer midplane edge was set equal to its value for the parameters of the base line CTF design ($N=10$, $R_{coil}=2.4$ m); for this $\delta$, Table I gives the computed loss rate for $N=8$, 14, and 20. The $\alpha$ particles were again simulated for $\approx 10^5$ Larmor orbits. One might have
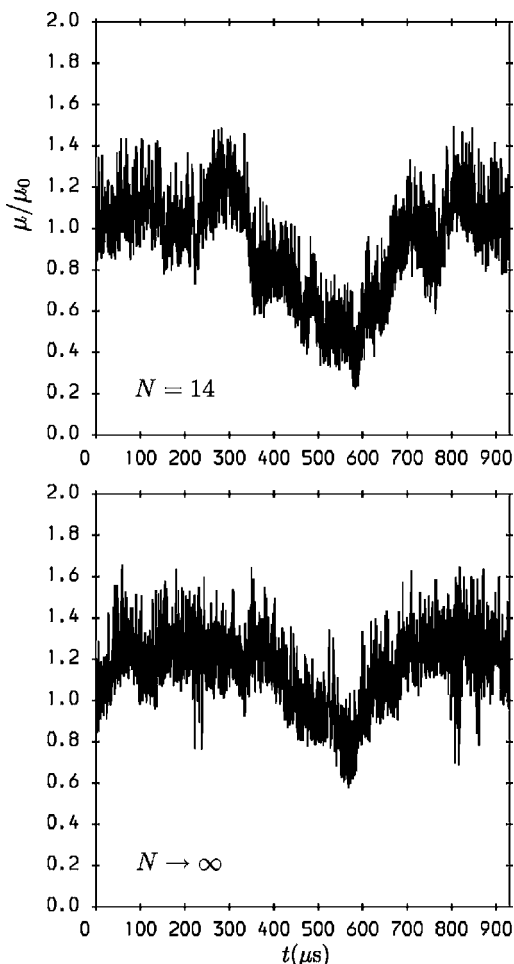
FIG. 9. Time variation of magnetic moment $\mu$ normalized to its initial value $\mu_0$ for a 3.5 MeV $\alpha$ particle lying close to the trapped-passing boundary in CTF, with $N=14$ (top) and $N \rightarrow \infty$ (bottom).

expected the losses to increase monotonically with $N$; in fact, the escape rate is lower for $N=14$ than it is for the other two cases. As $N$ is increased the ripple amplitude inside the plasma becomes a more strongly varying function of $R$, while at the same time finite Larmor radius effects become more significant. The computed variation of loss rate with $N$ may arise from competition between these two competing effects.

Tani and co-workers[9] have recently used a guiding center code to carry out a similar scan for VEry Compact TOkamak Reactor (VECTOR), a proposed low aspect ratio tokamak power plant.[8] Specifically, the power loss due to escaping $\alpha$ particles was computed as a function of $N$ with the ripple magnitude at the plasma edge held fixed at 1%.

TABLE I. Collisionless loss rate of $\alpha$ particles from CTF for three values of $N$, the ripple amplitude at the outer midplane plasma edge being held fixed.

| $N$ | Lost fraction of $\alpha$ particles (%) |
|---|---|
| 8 | $2.4 \pm 0.5$ |
| 14 | $1.4 \pm 0.4$ |
| 20 | $2.9 \pm 0.5$ |

Tani and co-workers found that the dependence of power loss on $N$ was very weak, and concluded from this that the number of toroidal field coils in VECTOR could be significantly reduced from that of the original design without causing unacceptable ripple losses. Such a reduction would, of course, have to be accompanied by an increase in the distance of the coils from the plasma, to ensure that the ripple amplitude at the plasma edge remained fixed.

## IV. DISCUSSION AND CONCLUSIONS

As noted in Sec. I, Putvinskii and Shurygin[14] proposed that fusion $\alpha$-particle transport could be enhanced if cyclotron resonance with the toroidal field ripple were to occur. Simple estimates indicate that the resonance condition would not be satisfied in ITER, at least as far as the lowest toroidal ripple harmonic is concerned. On the other hand, the condition would be marginally satisfied in STPP and easily satisfied in CTF. It is not clear, however, to what extent the predicted loss rates for either of these devices can be interpreted in terms of the Putvinskii and Shurygin model. Considering the case of a circular cross section, large aspect ratio tokamak, and retaining only leading order terms in the evolution equations for magnetic moment and gyrophase, Putvinskii and Shurygin deduced an area-preserving map representing the cyclotron interaction of $\alpha$ particles with a ripple field. Using this map, they showed that the threshold ripple amplitude for stochastic $\alpha$-particle transport tends to zero at the trapped-passing boundary. This is consistent with the demonstration by Yavorskij and co-workers[23] of nonadiabatic transitions from passing orbits to trapped orbits in the axisymmetric limit, and it is also consistent with the occurrence of stochastic variations in $\mu$ shown in Fig. 9. On the other hand, whereas in the Putvinskii and Shurygin model the volume of the stochastic region of phase space falls rapidly as the ripple amplitude is reduced, the computed CTF loss rates for $N=10$ and $N=20$ are similar (Fig. 7), despite a huge disparity in ripple amplitudes. Moreover, as noted previously, an increase in $N$ from 18 to 25 was found to have no significant effect on the loss rate in STPP.

In view of the qualitative similarity of the time series shown in the upper and lower frames of Fig. 9 (corresponding respectively to finite and infinite $N$), it seems likely that the delayed losses found in STPP and CTF for very high values of $N$ are due to violation of $\mu$ conservation in the axisymmetric component of the magnetic field, rather than ripple effects. Additional support for this conjecture lies in the fact that the normalized fusion $\alpha$-particle Larmor radius in both STPP and CTF is close to a threshold value above which strong collisionless pitch angle scattering is predicted to occur.[23] It is uncertain whether the occurrence of local minima in the collisionless loss rate for specific intermediate values of $N$ in STPP and CTF (Figs. 4, 5, and 7; Table I) is due specifically to finite Larmor radius effects. In any event, the existence of such minima is unlikely to be significant in terms of fusion $\alpha$-particle confinement in burning tokamaks. There are two reasons for this. First, as noted in Sec. III, the values of $N$ that yield improved confinement are profile dependent. Second, the fact that collisionless losses in STPP

and CTF are low in absolute terms for all values of $N$ above a certain minimum value suggests that the total loss rate is likely to be due mainly to collisional processes in such cases.

In conclusion, we have used a full orbit code to compute collisionless prompt and ripple losses of fusion $\alpha$ particles from three proposed burning tokamaks. For the inductive mode of operation in ITER (with magnetic shear increasing monotonically from the core to the edge), the scaling of loss rate with the number of toroidal field coils $N$ (and hence with the ripple amplitude) appears to be broadly consistent with that expected on the basis of guiding center theory. The introduction of higher spatial harmonics to the ripple field, representing the effects of ferromagnetic inserts, does not increase the loss rate. In the case of STPP and CTF, we have found that there is a range of values of $N$ for which the collisionless loss rate does not fall monotonically: within this range, there are specific values of $N$ for which collisionless losses drop to levels comparable to the prompt rate. Because of collisional effects (not considered in this paper), one would expect the actual loss rate in such cases to be considerably higher. As far as STPP and CTF are concerned, the key result emerging from the full orbit computations is that the collisionless loss rates are always low in absolute terms except for values of $N$ well below those of the base line designs. Our results imply that fusion $\alpha$-particle confinement would not be significantly degraded as a result of finite Larmor radius effects in any of the burning tokamaks considered in this paper.

## ACKNOWLEDGMENTS

[1] L. M. Hively, Fusion Technol. **13**, 438 (1988).
[2] L. M. Hively and J. A. Rome, Nucl. Fusion **30**, 1129 (1990).
[3] P. N. Yushmanov, Rev. Plasma Phys. **16**, 117 (1990).
[4] G. Kamelander, S. Putvinskij, V. Saplahidy, and A. Smirnov, *Plasma Physics and Controlled Nuclear Fusion Research 1990* (International Atomic Energy Agency, Vienna, 1991), Vol. 3, p. 533.
[5] S. Konovalov, T. Takizuka, K. Tani, K. Hamamatsu, and M. Azumi, JAERI-Research 94-033 (1994).
[6] M. H. Redi, R. V. Budny, D. C. McCune, C. O. Miller, and R. B. White, Phys. Plasmas **3**, 3037 (1996).
[7] S. V. Konovalov, E. Lamzin, K. Tobita, and Yu. Gribov, *Proceedings of the 28th EPS Conference on Controlled Fusion and Plasma Physics*, edited by C. Silva, C. Varandas and D. Campbell (European Physical Society, Petit-Lancy, 2001), Vol. **25A**, p. 613.
[8] S. Nishio, K. Tobita, K. Tokimatsu, K. Shinya, I. Senda, T. Isono, Y. Nakamura, M. Sato, S. Sakurai, M. Yamauchi, T. Nishitani, K. Tani, S. Sengoku, Y. Kudo, Y. Song, and S. Konishi, *Proceedings of the 20th IAEA Fusion Energy Conference* (International Atomic Energy Agency, Vienna, 2005), Invited Paper FT/P7-35.
[9] K. Tani, K. Tobita, S. Tsuji-Iio, H. Tsutsui, S. Nishio, and T. Aoki, "Confinement of alpha-particles in a low-aspect-ratio tokamak reactor," presented at the *Tenth International ST Workshop*, Kyoto, 29 September–1 October 2004.
[10] R. J. Goldston, R. B. White, and A. H. Boozer, Phys. Rev. Lett. **47**, 647 (1981).
[11] R. J. Goldston and H. H. Towner, J. Plasma Phys. **26**, 283 (1981).
[12] F. L. Hinton, Plasma Phys. **23**, 1143 (1981).
[13] S. V. Putvinskii, JETP Lett. **36**, 397 (1982).
[14] S. V. Putvinskii and R. V. Shurygin, Sov. J. Plasma Phys. **10**, 534 (1984).
[15] T. C. Hender, A. Bond, J. Edwards, P. J. Karditsas, K. G. McClements, J. Mustoe, D. V. Sherwood, G. M. Voss, and H. R. Wilson, Fusion Eng. Des. **48**, 255 (2000).
[16] H. R. Wilson, J.-W. Ahn, R. J. Akers, D. Applegate, A. Cairns, J. P. Christiansen, J. W. Connor, G. Counsell, A. Dnestrovskij, W. D. Dorland, M. Hole, N. Joiner, A. Kirk, P. J. Knight, C. N. Lashmore-Davies, K. G. McClements, D. E. McGregor, M. O'Brien, C. M. Roach, S. Tsaun, and G. M. Voss, Nucl. Fusion **44**, 917 (2004).
[17] H. R. Wilson, R. J. Akers, L. Appel, A. Dnestrovskij, T. C. Hender, G. T. A. Huysmans, A. Kirk, P. J. Knight, M. Loughlin, K. G. McClements, D. Yu. Sychugov, and G. M. Voss, *Proceedings of the 31st EPS Conference on Plasma Physics*, edited by P. Norreys and H. Hutchinson (EPS, Petit-Lancy, 2004), Vol. **28B**, P-4.196.
[18] H. R. Wilson, G. M. Voss, R. J. Akers, L. Appel, A. Dnestrovskij, O. Keating, T. C. Hender, M. J. Hole, G. Huysmans, A. Kirk, P. J. Knight, M. Loughlin, K. G. McClements, M. R. O'Brien, and D. Yu. Sychugov, *Proceedings of the 20th IAEA Fusion Energy Conference* (International Atomic Energy Agency, Vienna, 2005), Invited Paper FT/3-1Ra.
[19] B. Hamilton, K. G. McClements, L. Fletcher, and A. Thyagaraja, Sol. Phys. **214**, 339 (2003).
[20] W. A. Newcomb, Ann. Phys. (N.Y.) **10**, 232 (1960).
[21] H. R. Wilson, UKAEA Fusion Report No. FUS 271, 1994 (unpublished).
[22] H. Brysk, Plasma Phys. **15**, 611 (1973).
[23] V. A. Yavorskij, D. Darrow, V. Ya. Goloborod'ko, S. N. Reznik, U. Holzmüler-Steinacker, N. Gorelenkov, and K. Schöpf, Nucl. Fusion **42**, 1210 (2002).
[24] R. J. Hastie, G. D. Hobbs, and J. B. Taylor, *Proceedings of the 3rd IAEA Conference on Plasma Physics and Controlled Nuclear Fusion Research* (International Atomic Energy Agency, Vienna, 1969), Vol. **1**, p. 389.